XLIII CILAMCE
21–25, November, 2022
FOZ DO IGUAÇU – PR – BRAZIL

The importance of linear search for the bound-constrained solver for phase-field modeling of fracture in quasi-brittle materials with FEM

Matheus Moreno Fortes[1], Hugo Mouro Leão[1], Lapo Gori[1], Roque Luiz da Silva Pitangueira[1].

[1]*Structural Engineering Department at the Federal University of Minas Gerais*
Av. Antônio Carlos, 6627, Pampulha, 31270-901, Minas Gerais, Brazil
matheuseng97@gmail.com,hugomleao@yahoo.com.br,lapo@dees.ufmg.br,roque@dees.ufmg.br

Abstract. The propagation and emergence of cracks are widely explored in fracture mechanics. A study that has increased with the advancement of computer technology is the phase-field for crack modeling. This model approaches the crack as continuous and diffuse, placing a damage variable in the problem and a variable with the crack band size. There are different ways to control crack irreversibility, such as the bound-constrained solver and the historical solver. The bound-constrained solver allows you to choose any crack geometry function and energy degradation while the historical solver needs to be a specific crack geometry function. In this article, the importance of linear search for bound-constrained solver results will be discussed through numerical simulations, showing that the line search is necessary to avoid numerical instabilities as well as a correct load peak. Numerical simulations were processed in *INSANE* software (INteractive Structural ANalysis Environment). This work uses a bound-constrained solver from the PETSc library, connected to *INSANE* through a JNI.

Keywords: Phase-field model, bound-constrained solver, line search

1 Introduction

With the advent of computers, numerical simulations of structures could be performed, and with that, safer projects were made. Fracture mechanics benefited from this, being able to simulate the opening and propagation of cracks. There are two ways to model cracks: discretely and continuously. In continuous modeling there are several forms already established in the literature, and the phase-field is one of them.

The phase field model generalizes the Griffith theory, aiming to solve the displacement field and the fracture region by energy minimization and no assumptions for the evolution of the cracks are necessary (Goswami et al. [1]). The phase-field (ϕ) is a scalar variable that goes from 1 for the fully cracked state of the material to 0 for the undamaged state. In addition to the phase-field variable, another parameter is the length scale parameter (l_0), that controls the width of the region where the discrete crack is smoothed. Small values of this length tends to reproduce the Griffith's theory.

The phase-field has already been widely discussed by several authors. A complete review of this strategy, which addresses several references on the subject, can be found in Wu et al. [2]. In phase-field models, when dealing with the irreversibility of the crack, care must be taken, since when using the historical solver (Miehe et al. [3]), it limits the selection of the crack geometric function and the degradation energy function. One way to get around this problem is to use a bound-constrained solver

The computational implementations were done in the program *INSANE*[1] (INteractive Structural ANalysis Environment). This is an open-source program based on the Object-Oriented Programming paradigm and developed at the Department of Structural Engineering of the Federal University of Minas Gerais (Penna [6], Fuina [7]). It was used in this work the library PETSc (Portable, Extensible Toolkit for Scientific Computation) for the bound-constrained solver. PETSc is a suite of data structures and routines for the scalable (parallel) solution of scientific applications modeled by partial differential equations. In order to use PETSc, a binding was made (JNI - Java Native Interface) to `INSANE`, because `INSANE` is written in Java and PETSc written in C. In *INSANE* there are two such solvers implemented, one in the code itself (Bayao et al. [4]) and the other through the library PETSc (Fortes et al. [5]).

[1]The development code is available at the Git repository URL `http://git.insane.dees.ufmg.br/insane/insane.git`.

The objective of this work is to use the bound-constrained solver by PETSc to analyze the importance of using this solver with a linear search.

2 Phase-field modelling for fracture

In the phase-field model there is the a domain Ω, where a broken part $\mathcal{B} \subset \Omega$ is considered. $\mathcal{B}$ is the region where the fracture is located and smoothed by the phase-field model. The boundary of the solid and the broken surface are, respectively, $\partial\Omega$ and $\partial\mathcal{B}$.

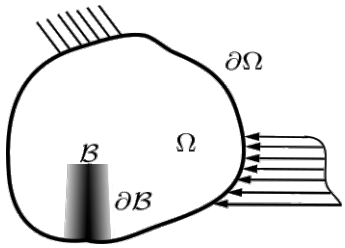

Figure 1. A solid body with a crack.

Within the phase-field approach, the total energy functional E_t is given by:

$$E_t = \int_\Omega \psi(\underline{\varepsilon}(\bar{u}), \phi)\ \mathrm{d}\mathcal{V} + \int_\mathcal{B} G_c \gamma(\phi, \nabla\phi)\ \mathrm{d}\mathcal{V} + -\int_\Omega \bar{b}\cdot\bar{u}\ \mathrm{d}\mathcal{V} - \int_{\partial\Omega} \bar{t}\cdot\bar{u}\ \mathrm{d}\mathcal{A} \tag{1}$$

where $\bar{u}$ is the displacements field, ϕ is the phase-field, ψ is the strain energy density (section 2.2), G_c is a material property that represents the critical energy release rate, γ is the crack surface density function (section 2.1), $\bar{b}$ are the body forces and $\bar{t}$ are the surface forces.

2.1 Crack Surface Density Function

The crack surface density function γ in eq. (1) describes how the sharp crack topology is smoothed over the domain. Wu [8] proposed a general equation for the surface density function of the crack:

$$\gamma(\phi, \nabla\phi) = \frac{1}{C_0}\left[\frac{1}{l_0}\alpha(\phi) + l_0 \mid \nabla\phi \mid^2\right] \tag{2}$$

where the *crack geometry function* $\alpha(\phi)$ and the parameter $C_0 = 4\int_0^1 \alpha^{1/2}(\phi)d\phi$ have been introduced. The function $\alpha(\phi)$ determines how the phase-field will be distributed and it has to satisfy the following properties: $\alpha(0) = 0$ and $\alpha(1) = 1$. Was proposed by Wu [8] the following quadratic equation for α:

$$\alpha(\phi) = \xi\phi + (1-\xi)\phi^2 \in [0,1] \quad \forall\phi \in [0,1] \tag{3}$$

where $\xi \in [0,2]$, otherwise $\alpha(\phi) \in [0,1]$ cannot be guaranted Wu et al. [2].

2.2 Energy Degradation Function

The energy degradation function $g(\phi)$, makes the connection between the crack phase-field and the mechanical fields. The strain energy function, in eq. (1), describes a smooth transition between the fully broken and fully unbroken states of the material. The *initial strain energy density function* $\psi_0(\underline{\varepsilon})$ and the degradation function $g(\phi) : [0,1] \longrightarrow [1,0]$ are used to describe the strain energy function.

An anisotropic formulation based on the following additive decomposition of the elastic strain energy is commonly adopted in the literature to prevent crack formation in compresion regions:

$$\psi_0(\underline{\varepsilon}) = \psi_0^+(\underline{\varepsilon}) + \psi_0^-(\underline{\varepsilon}) \tag{4}$$

where $\psi_0^+(\underline{\varepsilon})$ is the part that comes from tensile strains (active strain energy density) and $\psi_0^-(\underline{\varepsilon})$ is the part due to compressions (inactive strain energy density). The degradation is then assumed to affect just the tensile part:

$$\psi(\underline{\varepsilon}) = g(\phi)\psi_0^+(\underline{\varepsilon}) + \psi_0^-(\underline{\varepsilon}) \tag{5}$$

There are many energy degradation functions, already proposed in the literature. In this work the focus is the $g(\phi)$ function proposed by Wu [8]:

$$g(\phi) = \frac{(1-\phi)^p}{(1-\phi)^p + Q(\phi)} \tag{6}$$

where $p > 0$, and the continuous function $Q(\phi) > 0$ is given by:

$$Q(\phi) = c_1\phi + c_1c_2\phi^2 + c_1c_2c_3\phi^3 + \cdots \tag{7}$$

where c_1, c_2 and c_3 are given by:

$$c_1 = \frac{2E_0G_c}{f_t^2}\frac{\xi}{C_0l_0} = \frac{2\xi}{C_0}\frac{l_{ch}}{l_0} \tag{8}$$

$$c_2 = \frac{1}{\xi}[(-\frac{4\pi\xi^2}{C_0}\frac{G_c}{f_t^2}k_0) - (p+1)] \tag{9}$$

$$c_3 = \begin{cases} 0 \quad p > 2 \\ \frac{1}{c_2}[\frac{1}{\xi}(\frac{C_0w_cf_t}{2\pi G_c})^2 - (1+c_2)] \quad p = 2 \end{cases} \tag{10}$$

where E_0 is the Young´s modulus, f_t is the failure strength and $l_{ch} = E_0G_c/f_t^2$ is the characteristic length, for Griffith´s or Irwin´s theories. w_c is the ultimate apparent displacement jump (ultimate crack opening) and k_0 is the initial slope for the softening curves, which represent the relationship between the stress (σ) and the apparent displacement jump (w) across the localisation band. More details on the parameters w_c and k_0 can be found in Wu [8]. The values of w_c and k_0 can also be stipulated for certain softening laws already established in the literature (Wu [8]). In this work, the Cornelissen's softening law (Cornelissen et al. [9]) will be considered.

2.3 Equations of Phase-Field Models in Weak Form

The governing equations of a phase-field model in weak form are:

$$\begin{cases} \int_\Omega \underline{\sigma} : \delta\underline{\varepsilon} \ \mathrm{d}\mathcal{V} = \delta P_{ext} \\ \int_\mathcal{B} \left[g'(\phi)\bar{Y}\delta\phi + G_c\dfrac{1}{l_0}\alpha'(\phi)\delta\phi + 2l_0\nabla\phi\cdot\nabla\delta\phi \right] \ \mathrm{d}\mathcal{V} \geq 0 \end{cases} \tag{11}$$

where $\bar{Y} = \dfrac{\partial\psi}{\partial g}$ is the *effective crack driving force*. More details on the development of the equation can be found in Wu et al. [2] and Leão [10].

2.4 Hybrid Constitutive Model

Hybrid models were developed as an alternative to maintain the asymmetric behavior with respect to tension and compression, but at the same time avoiding excessive non-linearity caused by the definition of $\vec{Y}$ (*effective crack driving force*) by the part deformation energy, which makes solving the displacements little efficient in models that make separation of variables (Wu et al. [2]). In this work, the hybrid model based on the work of Wu [11] will be used, where $\psi_0 = \sigma_1^2/(2E_0)$, where σ_1 denotes the first major principle value of the effective stress $\underline{\sigma}$.

3 Bound-Constrained Solver for Phase-Field

3.1 Bound-Constrained Solver

To deal with the boundedness and irreversibility conditions, it's convenient to regard the governing equation from residual phase-field form as an optimization problem bounded by the following condition:

$$0 \leq a_{I,n} \leq a_{I,n+1} \leq 1 \tag{12}$$

where $\bar{a}$ is nodal phase-field, n is the current step, $n+1$ is the next step and I is the index for each node. The residual phase-field is obtained through the development of discretization by finite element method of phase-field in weak form (section 2.3), more details in Wu et al. [2]. The nodal phase-field is described by the relation $\phi(\bar{x}) = [\mathbf{N}]^\phi\,\bar{a}$, where $[\mathbf{N}]^\phi$ is the shape function for phase-field variable.

According to Farrell and Maurini [12], under the above condition the residual phase-field equation constitutes a mixed complementarity problem (MCP), which is a problem formulation in mathematical programming, that can be written as:

$$\begin{cases} a_{I,n} < a_{I,n+1} < 1 \quad r_I^{\phi} = 0 \quad \texttt{Inactive} \quad \texttt{set}(\mathscr{I}) \\ a_{I,n} = a_{I,n+1} \quad r_I^{\phi} \leq 0 \quad \texttt{Active} \quad \texttt{set}(\mathscr{A}) \\ a_{I,n+1} = 1 \quad r_I^{\phi} \geq 0 \quad \texttt{Active} \quad \texttt{set}(\mathscr{A}) \end{cases} \tag{13}$$

where r_I^{ϕ} is the residual phase-field. Equation 13 says that the solution of residual phase-field needs to be for each node, precisely, one of the conditions shown. We use a reduced-space active set Newton method, included in the the open-source toolkit PETSc (Balay et al. [13]), to solve this problem, just as Wu et al. [2] and Farrell and Maurini [12] did. In order to use PETSc, a binding was made to *INSANE*, because *INSANE* is written in Java and PETSc written in C. To do this, a Java Native Interface (JNI) was made based on Azevedo [14].

In the algorithm (Fig. 2) the active set is the subdomain with the restrictions applied and no equation is solved, while in the inactive set the equations are solved, in such way that the restrictions are satisfied. So the idea of the algorithm is to reduce the number of equations to be solved at each step, as it updates the inactive set. The indices i, j and k in Fig. 2 refer, respectively, to the step, global iteration and local phase-field iteration. In this article we use a staggered solver, which solves the phase-field and displacement separately.

while *phase-field doesn't converge* **do**
- (*INSANE*): Phase-field stiffness matrix: $[\mathbf{K}]_{i,j,k-1}^{\phi\phi}$
- (*INSANE*): Phase-field residue: $\vec{R}_{i,j,k-1}^{\phi}$
- (JNI): *INSANE* $\rightarrow$ PETSc
- (PETSc): Compute Active and Inactive sets
- (PETSc): Incremental phase-field: $([\mathbf{K}]_{i,j,k-1}^{\phi\phi})\delta\vec{a}_{i,j,k} = \vec{R}_{i,j,k-1}^{\phi}$
- (JNI): PETSc $\rightarrow$ *INSANE*
- (*INSANE*): Backtracking Armijo Line-search
- (*INSANE*): Update phase-field: $\vec{a}_{i,j,k} = \vec{a}_{i,j,k-1} + \delta\vec{a}_{i,j,k}$
- (*INSANE*): Verify local convergence for phase-field

end

Figure 2. Pseudocode for phase-field convergence with bound-constrained solver by PETSc.

3.2 Tolerances

As the solution to the problem is separated, a convergence is made for the phase-field and another for the displacements. In this work, two tolerances will be mentioned, a local and a global tolerance. Local tolerance refers to the separate convergence of displacement and phase-field variables, while the global tolerance checks if the displacement convergence, after the phase-field convergence, was not unbalanced, it would be a local displacement tolerance after the phase-field convergence. The local convergence is reached when the error calculated by

$$\text{Error} = \frac{\left\|\delta\vec{X}\right\|}{\left\|\vec{X}\right\|} \tag{14}$$

is smaller then a defined tolerance, where $\delta\bar{X}$ and $\bar{X}$ can be the residual load and the forces vector, or the incremental displacements and the displacements vector, depending on the convergence type Leão et al. [15].

In this work, the line search for the bound-constrained solver will be investigated, therefore, another convergence for the local phase-field iteration will be investigated, which is due to a restrict operator given by eq. (15).

$$F_{\Theta}(\bar{a}_{n+1})_I = \begin{cases} r_I^{\phi}, \text{for } a_{I,n} < a_{I,n+1} < 1 \\ \min(r_I^{\phi}, 0), \text{for } a_{I,n+1} = 1 \\ \max(r_I^{\phi}, 0), \text{for } a_{I,n} = a_{I,n} \end{cases} \tag{15}$$

Where the convergence of the iteration is given by $||\bar{F_{\Theta}}(\bar{a}_n^k + 1)|| > TOL$. More details on this convergence, can be found in Bayão [16] and Bayao et al. [4].

4 Numerical Examples

The purpose of this section is to show the importance of the line search and some findings about its use with convergences. In this entire section the same data will be used for two different examples. The following data were used: $E_0 = 25850$ N/mm^2, Poisson´s ratio $\nu = 0.18$, $f_t = 2.7$ MPa, $G_c = 0.065$N/mm, $l_0 = 8.5$ mm, Cornelissen's softening law for normal concrete (η_1 = 3 and η_2 = 6.93) and hybrid constitutive model stated in section 2.4. Data were taken from the numerical L-Shaped Panel model from Penna [17]. In all examples displacement control was used, the local tolerance used was of $1 \cdot 10^{-4}$ and the global tolerance was of $1 \cdot 10^{-4}$. All cases are in a plane stress.

Furthermore, in this section there will be the same model processed with different conditions of the solvers, where each processing is described below:

- Processing 1 - Bound-constrained solver in *INSANE* (Bayao et al. [4]) with line search and $||\bar{F_\Theta}(\bar{a}_n^k + 1)||$ convergence
- Processing 2 - Bound-constrained solver by PETSc (Fortes et al. [5]) with line search and $||\bar{F_\Theta}(\bar{a}_n^k + 1)||$ convergence
- Processing 3 - Bound-constrained solver by PETSc without line search and $\left\|\delta\bar{X}\right\| / \left\|\bar{X}\right\|$ convergence
- Processing 4 - Bound-constrained solver by PETSc with line search and $\left\|\delta\bar{X}\right\| / \left\|\bar{X}\right\|$ convergence
- Processing 5 - Bound-constrained solver by PETSc with line search and $||\bar{F_\Theta}(\bar{a}_n^k + 1)||$ convergence and and half the step size

4.1 Uniaxial Traction Test

The first result will be based on a numerical uniaxial traction model of a quadrilateral element with side of 1 mm with only one element Q4. Increments of $2 \cdot 10^{-5}$ were considered in all cases. The results for the load versus horizontal displacement for each processing are shown in Fig. 3.

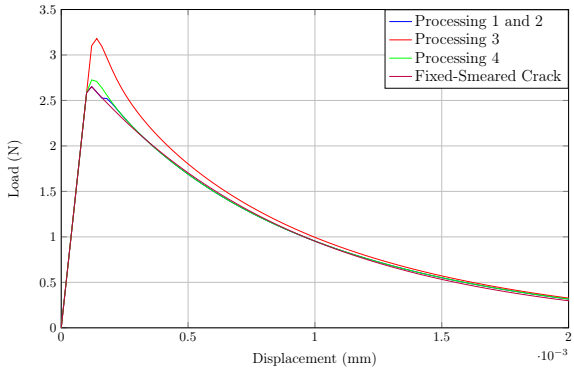

Figure 3. Curves of load versus displacement for Uniaxial Traction Test

Analyzing the Fig. 3, it is noted that when the line search is not used, the bound-constrained solver presents a peak load far from the reference, which is the result of a generalized fixed-smeared crack model implemented in *INSANE* by Penna [17]. It is also noted that despite using the bound-constrained with line search and with $\left\|\delta\bar{X}\right\| / \left\|\bar{X}\right\|$ convergence, the peak load is already very close to what was expected. And the best result is for the bound-constrained solver with $||\bar{F_\Theta}(\bar{a}_n^k + 1)||$ convergence.

4.2 L-Shaped Panel

The second result will be based on the L-Shaped Panel shown in Fig. 4a with measurements in millimeters. A vertical point load F is applied upward at a distance of 30mm to the right edge of the horizontal leg, with the corresponding vertical displacement at the same place recorded. The mesh used is formed by CST (Constant strain triangle element) elements, shown in Fig. 4b. Increments of $2 \cdot 10^{-3}$ were considered in all cases. The results for the load versus vertical displacement of the point where the load is applied for each processing are shown in Fig. 5.

Analyzing Fig. 5, it is noted that when the line search is not used, the bound-constrained solver presents a load

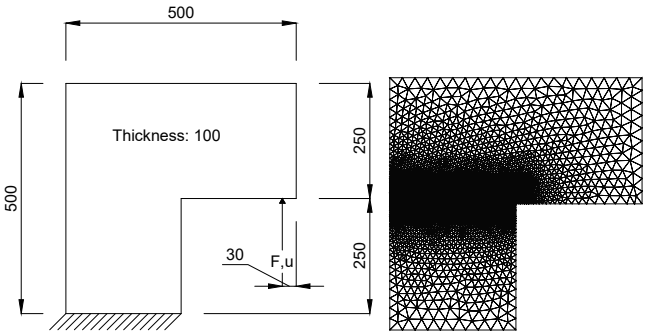

(a) (b)

Figure 4. L-Shaped Panel. (a) Problem setting.(b) T3 mesh ($h = 25$ mm in the unrefined region and $h = 4$ mm in the refined region)

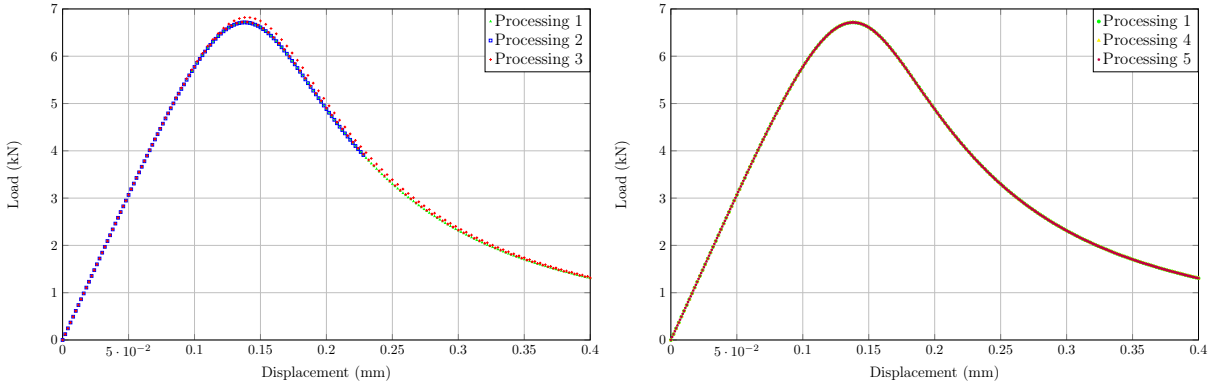

(a) (b)

Figure 5. Curves of load versus displacement for L-Shaped Panel

peak a little far from the reference, and the result presents numerical instability. When using the bound-constrained solver with line search solver and with $\left\|\delta\bar{X}\right\| / \left\|\bar{X}\right\|$ convergence, the peak load is within the expected range and there is no numerical instability. When using the bound-constrained solver with line search and $||\bar{F}_\Theta(\bar{a}_n^k + 1)||$ convergence, not all results are processed, only when the step is reduced to half the step (increments of $1 \cdot 10^{-3}$, doubling the number of necessary steps - Processing 5) that all the desired results are obtained.

4.3 Discussions

Although the type of convergence changed the result a little for line search, the two shown did not change the result significantly. In addition, it can be seen that for $||\bar{F}_\Theta(\bar{a}_n^k + 1)||$ convergence, perhaps there will be no results from a certain step, so it is necessary to reduce the step size for the imposed displacement (since the displacement control method was used), until it can be processed. It is worth mentioning that an Bactracking Armijo was used for the linear search, so other types of searches may present better results.

5 Conclusion

In this article, the phase-field theory and a bound-constrained solver were briefly presented. Later, the importance of linear search for a bound-constrained solver through numerical models was shown. In addition, the analysis showed that depending on the convergence, the results can be slightly altered, as well as not being able to obtain them, requiring a reduction in the step size.

Acknowledgements. The authors gratefully acknowledge the support from the Brazilian research agencies CAPES (*Coordenação de Aperfeiçoamento de Pessoal de Nível Superior*), FAPEMIG (*Fundação de Amparo à Pesquisa do Estado de Minas Gerais*; Grant PPM-00747-18) and CNPq (*Conselho Nacional de Desenvolvimento Científco e Tecnológico*; Grant 316240/2021-4).

Authorship statement. The authors hereby confirm that they are the sole liable persons responsible for the authorship of this work, and that all material that has been herein included as part of the present paper is either the property (and authorship) of the authors, or has the permission of the owners to be included here.

References

[1] S. Goswami, C. Anitescu, and T. Rabczuk. Adaptive fourth-order phase field analysis for brittle fracture. *Computer Methods in Applied Mechanics and Engineering*, vol. 361, pp. 112808, 2020.
[2] J.-Y. Wu, V. P. Nguyen, C. Thanh Nguyen, D. Sutula, S. Bordas, and S. Sinaie. Chapter One - Phase-field modeling of fracture. *Advances in Applied Mechanics*, vol. 53, pp. 1–183, 2020.
[3] C. Miehe, M. Hofacker, and F. Welschinger. A phase field model for rate-independent crack propagation: Robust algorithmic implementation based on operator splits. *Computer Methods in Applied Mechanics and Engineering*, vol. 199, pp. 2765–2778, 2010b.
[4] R. Bayao, H. M. Leao, M. M. Fortes, R. L. S. Pitangueira, and L. G. Gori. Implementation of bound-constrained solver in phase-field modeling of fractrure. In *Proceedings of 42nd Ibero-Latin-American Congress on Computational Methods in Engineering (XLII CILAMCE) and 3rd Pan American Congress on Computational Mechanics (III PANACM)*, 2021.
[5] M. M. Fortes, H. M. Leao, R. Bayao, R. L. S. Pitangueira, and L. G. Gori. A bound-constrained solver for phase-field modelling of diffuse fracture. In *Proceedings of 42nd Ibero-Latin-American Congress on Computational Methods in Engineering (XLII CILAMCE) and 3rd Pan American Congress on Computational Mechanics (III PANACM)*, 2021.
[6] S. S. Penna. Pós-processador para modelos bidimensionais não-lineares do método dos elementos finitos. Master dissetation, Universidade Federal de Minas Gerais (UFMG). (in portuguese), 2007.
[7] J. S. Fuina. Métodos de controle de deformações para análise nao-linear de estruturas. Master dissetation, Universidade Federal de Minas Gerais (UFMG). (in portuguese), 2004.
[8] J.-Y. Wu. A unified phase-field theory for the mechanics of damage and quasi-brittle failure. *Journal of the Mechanics and Physics of Solids*, vol. 103, pp. 72–99, 2017.
[9] H. A. W. Cornelissen, D. A. Hordijk, and H. W. Reinhardt. Experimental determination of crack softening characteristics of normalweight and lightweight concrete. *Heron*, vol. 31, n. 2, pp. 45–56, 1986.
[10] H. M. Leão. A critical study on phase-field modeling of fracture. Master dissetation, UFMG - Universidade Federal de Minas Gerais, Belo Horizonte, MG, Brasil, 2021.
[11] J.-Y. Wu. Robust numerical implementation of non-standard phase-field damage models for failure in solids. *Computer Methods in Applied Mechanics and Engineering*, vol. 340, pp. 767–797, 2018.
[12] P. Farrell and C. Maurini. Linear and nonlinear solvers for variational phase-field models of brittle fracture. *International Journal for Numerical Methods in Engineering*, vol. 109, n. 5, pp. 648–667, 2017.
[13] S. Balay, S. Abhyankar, M. F. Adams, J. Brown, P. Brune, K. Buschelman, L. Dalcin, A. Dener, V. Eijkhout, W. D. Gropp, D. Karpeyev, D. Kaushik, M. G. Knepley, D. A. May, L. C. McInnes, R. T. Mills, T. Munson, K. Rupp, P. Sanan, B. F. Smith, S. Zampini, H. Zhang, and H. Zhang. PETSc users manual. Technical Report ANL-95/11 - Revision 3.14, Argonne National Laboratory, 2020.
[14] G. M. Azevedo. Implementação paralela para analises estáticas lineares pelo métodos dos elementos finitos. Master dissetation, UFMG - Universidade Federal de Minas Gerais, Belo Horizonte, MG, Brasil, 2019.
[15] H. M. Leão, R. L. S. Pitangueira, L. Gori, and S. Penna. Phase-field modelling of size effect on strength and structural brittleness. *J Braz. Soc. Mech. Sci. Eng.*, vol. 43,484, 2021.
[16] R. Bayão. Estudo de modelos de campo de fase para análise de fratura. Monografia (Engenharia Mecânica), UFMG (Universidade Federal de Minas Gerais), Belo Horizonte, MG, Brazil, 2021.
[17] S. S. Penna. *Formulação multipotencial para modelos de degradação elástica: unificação teórica, proposta de novo modelo, implementação computacional e modelagem de estruturas de concreto*. Phd thesis, Universidade Federal de Minas Gerais (UFMG). (in portuguese), 2011.